Silica-Based Nanoparticles Targeting Dendritic Cells for Cancer Immunotherapy

Yajing Liu
Zhengzhou University
Lintong Yao
Zhengzhou University
Yun Zhang
zhengzhou university
Wenhui shen
Zhengzhou University
Chunxia Chen
Zhengzhou University
Hongfei Wang
Zhengzhou University
Yanfeng Gao
Zhengzhou University
Yuanming Qi
Zhengzhou University
Zhenzhen Chen (chenzz2015@zzu.edu.cn)
Zhengzhou University

Research

Keywords: Nanoparticle, dendritic cells, tumor vaccination, anti-tumor immunotherapy

DOI: https://doi.org/10.21203/rs.3.rs-87251/v1

Abstract

Background

Vaccination is a promising anticancer strategy, but the limited delivery routes and short retention of antigens and immunomodulatory agents are problems that need to be solved in vaccine design. Because silicon nanoparticles have a tunable pore size and high loading capacity, they have been used in a variety of drug delivery systems, but their roles in tumor vaccine and tumor immunotherapy need to be examined.

Methods

CD40 mAb was attached to mesoporous silica nanoparticles (MSNs) through covalent conjunction, and MSN-CD40/OVA/CpG nanoparticles were examined by Fourier transform-infrared spectroscopy, transmission electron microscopy and nanoparticle analyzer. In vitro functions of nanoparticles were detected by cytotoxicity, cellular uptake, DC maturation, cross-presentation and T cell priming. In vivo functions were monitored by tumor elimination, DC maturation, cross-presentation and T cell activity.

Results

We encapsulated anti-CD40 monoclonal antibodies, ovalbumin (OVA) antigen, and a toll-like receptor-9 agonist (CpG) in mesoporous silica nanoparticles (MSNs). The resulting MSN-CD40/OVA/CpG nanoparticles were efficiently phagocytized by splenocytes and bone marrow-derived dendritic cells (BMDC). The MSN-CD40/OVA/CpG nanoparticles induced the BMDC to express the costimulatory molecules CD80 and CD86, and release tumor necrosis factor-α. We found that MSN-CD40/OVA/CpG nanoparticles correctly enhanced antigen cross-priming, and stimulated T cell proliferation and interferon γ (IFNγ) production in vitro. In vivo, the MSN-CD40/OVA/CpG nanoparticles strongly increased intracellular IFNγ secretion and its release from $OVA_{257-264}$ peptide-specific splenocytes into the cell supernatant, induced dendritic cell expression of major histocompatibility complex-II, and stimulated lymphocyte CD80 and CD86 expression. The MSN-CD40/OVA/CpG nanoparticles also inhibited tumor growth, enhanced tumor infiltration of $CD8^+$ and $CD4^+$ T cells, and stimulated IFNγ secretion from splenocytes. In conclusion, we believe these MSN-CD40/OVA/CpG nanoparticles are a promising strategy for improving antigen cross-presentation, cytotoxic T lymphocyte immune activity, and anti-tumor immunotherapy.

Highlights

Mesoporous silica nanoparticle (MSN) is an excellent drug delivery and tumor vaccine system for anti-tumor immunotherapy.

MSN-based nanoparticles can be functionally extended by adding different modules (herein are CpG, OVA and anti-CD40 monoclonal antibody).

MSN-CD40/OVA/CpG nanoparticles are a promising strategy for improving antigen cross-presentation, cytotoxic T lymphocyte immune activity, and anti-tumor immunotherapy.

1. Introduction

Tumor immunotherapy has provided impressive results in animal models of human diseases, such as prostate cancer, colon cancer, and breast cancer, as well as in human clinical studies.[1, 2] The main purpose of therapeutic vaccines is to eliminate the cause of a given disease. Their activity is dependent on the induction of antigen-specific $CD8^+$ T cells to generate cytotoxic T lymphocytes (CTLs) primed to reject cancerous or infected cells.[3] Dendritic cells (DCs) are specific antigen-presenting cells in the immune system that capture the antigen and present the peptide to active $CD8^+$ T cells.[4] However, the infectious pathogens or cancerous cells may escape from immune surveillance and induce immune tolerance,[5] and the generation of robust CTL in vivo remains a major challenge. CD40 is a promising target on DCs for cancer immunotherapy.[6] In patients with advanced solid malignancies, CD40 agonists showed antitumor activity and had a controlled toxicity profile. CD40 is a member of the tumor necrosis factor (TNF) family of cell-surface receptors that is highly expressed on DCs. Binding of CD40 to its receptor on DCs enhances the expression of costimulatory mediators, such as CD80 and CD86, and major histocompatibility complex (MHC) molecules, and induces the release of immune-stimulatory cytokines.[7] It also plays a vital role in the maturation of DCs into fully competent antigen-presenting cells (APCs) and is a key signal for $CD4^+$ T helper-dependent $CD8^+$ T cell priming.[8, 9] Immature DCs express pathogen recognition receptors, such as toll-like receptors (TLR), to control the danger signals capable of stimulating the innate immune system.[10]

Many types of engineered materials have been developed and their potential immunomodulatory properties have been evaluated in several platforms, including poly(lactide-co-glycolide) nanoparticles,[11-13] gold nanoparticles,[13, 14] liposomes,[15-17] mesoporous silica,[18-20] and other materials.[21-24] Mesoporous silica nanoparticles (MSNs), which have a distinctive mesoporous structure, good biocompatibility, and a large surface area, have attracted much attention for their potential biomedical applications.[25] Moreover, some antibody constructs have been developed that can encourage antigen internalization in early endosomes[26] and promote antigen-specific T cell responses.[27] Despite the advantages of anti-CD40 antibodies,[28, 29] there are many adverse side effects, such as vascular leakage, cytokine release syndrome,[30] and liver damage.[31]

In this study, we evaluated the use of MSN-CD40/ovalbumin (OVA)/TLR9 agonist (CpG) nanoparticles (Scheme 1) to facilitate the delivery of an antigen to DCs in vitro and induce DC maturation. Vaccination with the MSN-CD40/OVA/CpG nanoparticles elicited a robust antigen-specific $CD8^+$ T cell response, controlled tumor growth, and had low toxicity in vivo.

2. Materials And Methods

2.1 Materials and animals

OVA, 3-[4,5-dimethyl-2-thiazolyl]-2,5-diphenyl-2H-tetrazolium bromide (MTT), fluorescein 5(6)-isothiocyanate (FITC), and MSNs were purchased from Sigma-Aldrich (St. Louis, MO, USA). CpG-ODN1826 (5'-TCCATGACGTTCCTGACGTT-3'–phosphonothioate) was synthesized by Genewiz (Suzhou, China). Bicinchoninic acid protein assay kits were purchased from Applygen (Beijing, China). Anti-mouse monoclonal antibodies (mAb) for flow cytometry (CD45, CD3, F4/80, B226, CD19, CD11b, CD11c, CD80, CD86, MHC-II, and CD8α) and APC-conjugated anti-mouse interferon γ (IFNγ) antibodies were purchased from eBioscience (San Diego, CA, USA). Granulocyte macrophage colony stimulating factor (GM-CSF) and interleukin (IL)-4 were purchased from PeproTech (Cranbury, NJ, USA). Hoechst 33342 and LysoTracker Red DND-99 were purchased from Invitrogen (Carlsbad, CA, USA) and Solarbio (Beijing, China), respectively. The EasySep mouse $CD8^+$ T cell isolation kit (negative selection) was purchased from STEMCELL Technologies (Vancouver, Canada). Enzyme-linked immunosorbent assays (ELISA) for TNFα and IFNγ were purchased from Invitrogen. The murine agonistic αCD40 mAb (FGK45) and mouse IgG2a isotype control were purchased from BioCell (Irvine, CA, USA). Red blood cell lysis solution was purchased from Thermo Fisher Scientific (Waltham, MA, USA). OVA-specific T cell receptor (TCR) transgenic mice (OT-I mice) and B16-OVA cells were kindly provided by Prof. Shengdian Wang (Institute of Biophysics, Chinese Academy of Sciences, Beijing, China). Female C57BL/6 mice were purchased from Vital River Laboratory (Beijing, China). All mice were housed in a specific pathogen-free facility.

2.2 Synthesis of CD40 mAb-engineered MSNs

CD40 mAb was covalently attached to the surface of the MSN-NH_2 particles using 1-ethyl-3-(3-dimethylaminopropyl)carbodiimide (EDC) coupling chemistry. CD40 mAb-bound EDC (120 μg, final concentration 2mM) and *N*-hydroxysuccinimide (final concentration 5 mM) were dissolved in 0.1 M MES buffer (pH 6.0) for 15 min at room temperature. Simultaneously, MSN-NH_2 particles (3 mg) were dispersed in phosphate-buffered saline (PBS; 100 mL, pH 8.5). The two solutions were mixed together for 2 h at room temperature. The MSN-CD40 nanoparticles were washed three times with PBS (pH 7.4) at 12,000 rpm. The nanoparticles were collected in KBr pellets, and the morphology and size of the nanoparticles were analyzed by Fourier transform-infrared spectroscopy (FT-IR; Nicolet iS 50; Thermo Fisher Scientific) and transmission electron microscopy (TEM; JEOL JEM-200CX, Japan) at 200 kV, respectively. The zeta potentials and hydrodynamic sizes of MSN-CD40/OVA/CpG nanoparticles and the controls were measured using a nanoparticle analyzer (Nano-ZS90, Malvern Instruments Co., Ltd., Malvern, UK).

2.3 Evaluation of cytotoxicity

C57BL/6 mice (6–8 weeks old) were sacrificed by cervical dislocation, the tibiae of hind limbs and intact femurs were removed using surgical instruments. The bones were washed in PBS (pH 7.4) and bone marrow was flushed with PBS (pH 7.4) using a syringe. Clusters within the bone marrow were disaggregated using red blood cell lysis solution to yield a homogeneous cell suspension. The cells were

seeded in a 100-mm bacteriological Petri dish in 20 mL of RPMI 1640 media containing 10% fetal bovine serum (FBS), 20 ng/mL GM-CSF, and 5 ng/mL IL-4 on day 0. Three days later, half of the media was replaced with fresh RPMI 1640 media containing the same concentrations of GM-CSF and IL-4. Cells were maintained in a humidified incubator at 37 °C and 5% CO_2. Bone marrow-derived dendritic cell (BMDC) viability was measured by the MTT assay. Briefly, BMDCs (5×10^4 cells) were seeded in a 96-well plate and incubated with MSN-CD40/OVA/CpG nanoparticles and appropriate controls (OVA/CpG and MSN-IgG/OVA/CpG, MSN/OVA/CpG nanoparticles), diluted to a concentration of 12.5 μg/mL OVA, for 24 h. After removing the supernatant, 20 μL of MTT (0.5 mg/mL in fresh RPMI-1640) was added to each well for 4 h at 37 °C, after which the medium was removed and dimethyl sulfoxide was added to solubilize the formazan. The absorbance of each well was measured at 560 nm.

2.4 Evaluation of cellular uptake

The intracellular uptake of FITC-labeled OVA by mouse splenocytes was determined by flow cytometry. Splenocytes (2×10^6 cells/well) were seeded onto a 24-well plate and subsequently incubated with fluorescently labeled OVA, using MSN-CD40/OVA-FITC/CpG nanoparticles or appropriate controls (OVA-FITC/CpG and MSN-IgG/OVA-FITC/CpG and MSN/OVA-FITC/CpG nanoparticles) at a final OVA-FITC concentration of 12.5 μg/mL, and incubated for 4 h at 37 °C. The cells were washed with cold PBS (pH 7.2) and stained with murine anti-CD45, anti-B220, anti-CD19, anti-CD11c, anti-F4/80, and anti-CD11b mAb to gate B cells, DC, and macrophages. We also incubated immature BMDC (4×10^6 cells/wells on six-well plates) in the same way and, after washing with cold PBS (pH 7.2), the cells were collected and stained with anti-CD11c mAb to test their uptake ability by flow cytometry. To investigate the uptake mechanism, immature BMDC (4×10^6 cells/well) were planted in six-well plates at 37 °C in the presence of genistein (50 μg/mL) and chlorpromazine (10 μg/mL) for 1 h before incubation with fluorescently labeled OVA in MSN-CD40/OVA-FITC/CpG nanoparticles.

2.5 Confocal imaging

To explore the localization of nanoparticles in DC, immature BMDC (4×10^6 cells/well) were plated onto 24-well plates at 37 °C, stained with LysoTrackerRed and Hoechst 33342, and fixed with paraformaldehyde. The cells were then analyzed by confocal laser scanning microscopy (TCS SP8, Leica, Wetzlar, Germany).

2.6 Maturation and cytokine detection in vitro

Immature BMDCs (2×10^5 cells/well) were seeded onto a 96-well plate and incubated for 24 h with MSN-CD40/OVA/CpG nanoparticles and appropriate controls (OVA/CpG and MSN-IgG/OVA/CpG and MSN/OVA/CpG nanoparticles) at a final OVA concentration of 12.5 μg /mL. The culture supernatant was removed and stained with anti-CD11c, anti-CD80, and anti-CD86 mAbs for 30 min on ice. The fluorescence markers expressed on the surface of BMDCs were measured by flow cytometry. The culture medium was collected to measure TNFα levels using an ELISA kit.

2.7 In vitro cross-presentation and T cell priming

Immature BMDCs (1×10^6 cells/well) were seeded onto a 96-well U-bottom plate and incubated for 4 h with MSN-CD40/OVA/CpG nanoparticles and appropriate controls (OVA/CpG and MSN-IgG/OVA/CpG and MSN/OVA/CpG nanoparticles) at a final OVA concentration of 12.5 μg/mL. $CD8^+$ T cells were negatively isolated from the lymphocytes of OT-I mice using a mouse $CD8^+$ T cell isolation kit and stained with 2 μM carboxyfluorescein succinimidyl ester (CFSE) for 10 min, after which cells were washed twice with culture medium. Next, $CD8^+$ T cells (1×10^5 cells/well) were seeded onto a 96-well U-bottom plate and cocultured with BMDC (1×10^4 cells/well) for 72 h. The culture medium was collected and the mixed cells were stained with anti-CD8 mAb for flow cytometry. The IFNγ concentration was also measured using an ELISA kit.

2.8 Animal immunization and CTL priming

C57BL/6 mice (6–8 weeks old) were immunized three times at 1-week intervals (n = 5 per group) with saline, OVA/CpG, MSN/OVA/CpG, MSN-IgG/OVA/CpG, or MSN-CD40/OVA/CpG with final concentrations of OVA and CpG of 100 and 30 μg per mouse, respectively. Five days after the last immunization, the immunized mice were sacrificed and the splenocytes were re-stimulated with $OVA_{257-264}$ peptide for 6 h or 5 days at 37 °C in vitro to acquire CTL effectors. The proportion of IFNγ-secreting activated cytotoxic $CD8^+$ T cells of splenocytes was analyzed by flow cytometry. IFNγ production was measured using an ELISA kit. To analyze DC maturation markers in the lymphocytes after administration of MSN-CD40/OVA/CpG or appropriate controls, the lymphocytes were stained with murine anti-CD45, anti-CD3, anti-CD11c, anti-CD80, anti-CD86, and anti-MHC-II mAb for 30 min on ice, washed with cold PBS, and analyzed by flow cytometry.

2.9 In vivo tumor challenge

B16-OVA cells were cultured in 100 mm cell culture dishes containing RPMI 1640 media with 10% FBS, 100 U/mL penicillin G, and 100 μg/mL streptomycin sulfate. Next, 2×10^5 B16-OVA melanoma cells were injected subcutaneously into the tail base of C57BL/6 mice, which were then immunized three times at 1-week intervals (n = 5 per group). After 3 days, the mice were subcutaneously injected with saline, OVA/CpG, MSN/OVA/CpG, MSN-IgG/OVA/CpG, or MSN-CD40/OVA/CpG, as appropriate. The final doses of OVA and CpG were 100 and 30 μg per mouse, respectively. The tumor size and body weight were measured every 2 days. Five days after the last immunization, the mice were sacrificed to detect tumor-infiltrating T cells. Tumor tissues were cut into small pieces and stained with murine anti-CD45, anti-CD3, anti-CD4, and anti-CD8 mAb for flow cytometry. After the splenocytes and lymphocytes were cultured with brefeldin A and $OVA_{257-264}$ peptide at a final concentration of 10 μg/mL, the cells were collected to measure intracellular IFNγ production by flow cytometry. The heart, liver, kidneys, and tumor were harvested and fixed in 4% paraformaldehyde for histopathological examination.

2.10 Statistical analysis

Data are presented as the mean ± standard deviation (SD) unless otherwise stated. Student's *t* test was used to determine the statistical significance of differences among the groups. $P < 0.05$ was considered statistically significant.

3. Results

3.1 Characterization of the nanoparticles

TEM images of the MSNs, MSN/OVA/CpG, and MSN-CD40/OVA/CpG revealed that the nanoparticles were monodispersed with a spherical morphology and a diameter of approximately 120 nm. The modification on the MSN surface was detected by FT-IR. The characteristic absorption peaks at 1689 and 1580 cm^{-1} arose from the amido band. The zeta potential was determined by dynamic light scattering (DLS). The sizes of the MSN-CD40/OVA/CpG nanoparticles in PBS did not change significantly, indicating their excellent stability (Fig. 1). Therefore, our results demonstrate that it is feasible to use MSN-CD40/OVA/CpG to deliver an antigen into DCs.

3.2 MSN-CD40/OVA-FITC/CpG improve internalization by DCs in vitro

The capability of splenocytes and BMDCs to internalize fluorescently labeled OVA via MSN-CD40/OVA-FITC/CpG nanoparticles was tested by flow cytometry. The MSN-CD40/OVA-FITC/CpG nanoparticles significantly improved the uptake of OVA by different subsets of splenocytes (Fig. 2). The $CD45^+CD11c^+$ DC and $CD45^+B220^+CD19b^+$ B cells internalized MSN-CD40/OVA/CpG nanoparticles more efficiently than $CD45^+CD11b^+F4/80^+$ macrophages. The MSN-CD40/OVA-FITC/CpG nanoparticles also enhanced the uptake of OVA by BMDCs (Figs. 3A,B). To explore the mechanism involved in BMDC uptake of MSN-CD40/OVA-FITC/CpG nanoparticles, the cells were treated with genistein, a caveolae inhibitor, to inhibit endocytosis or chlorpromazine to inhibit clathrin-mediated endocytosis. The results showed that the uptake efficiency of MSN-CD40/OVA-FITC/CpG nanoparticles was reduced by chlorpromazine. In contrast, genistein elicited a non-significant reduction in FITC fluorescence, which suggests that multiple endocytic pathways are involved in the internalization of CD40/OVA-FITC/CpG nanoparticles (Figs. 3C,D). Confocal fluorescence microscopy clearly showed intracellular green fluorescence, suggesting that FITC-labeled OVA was taken up by the BMDCs. The red fluorescence corresponding to LysoTracker Red further confirmed that MSN-CD40/OVA-FITC/CpG nanoparticles were internalized by BMDCs (Fig. 4). These results indicate that the MSN-CD40/OVA-FITC/CpG nanoparticles improved the uptake and delivery of CD40-targeting nanoparticles to DCs in vitro.

3.3 MSN-CD40/OVA/CpG nanoparticles enhanced the activation of DCs and antigen cross-presentation in vitro

The ability to promote DC maturation is an essential requirement of nanovaccines. Therefore, we evaluated the effects of the nanovaccine on DC maturation in vitro. The expression levels of CD80 and CD86 indicated that MSN-CD40/OVA/CpG nanoparticles more effectively induced BMDC maturation compared with MSN-IgG/OVA/CpG, MSN-IgG/OVA/CpG, MSN/OVA/CpG, and OVA/CpG nanoparticles (Figs. 5A,B). We also measured TNFα secretion into the culture medium by ELISA, and the results showed that the MSN-CD40/OVA/CpG nanoparticles enhanced cytokine release (Fig. 5C). The MTT assay showed that the MSN-CD40/OVA/CpG and other nanoparticles were not cytotoxic (Fig. 5D). To investigate the capacity of BMDCs on inducing $CD8^+$ T cell responses, we isolated lymph node $CD8^+$ T cells from OT-I mice and labeled the cells with 2 μM CFSE. Flow cytometry revealed that the MSN-CD40/OVA/CpG nanoparticles slightly induced $CD8^+$ T cell proliferation, but markedly promoted $CD8^+$ T cell activation, resulting in high IFNγ secretion (Fig. 6). These findings demonstrate that the MSN-CD40/OVA/CpG nanoparticles can induce BMDC maturation and promote antigen-specific $CD8^+$ T cell functionality.

3.4 Effects of MSN-CD40/OVA/CpG nanoparticles on immune responses in vivo

To explore the effects of MSN-CD40/OVA/CpG nanoparticles on immune responses in vivo, we used C57BL/6 mice as the immune model. After three subcutaneous injections, the frequency of IFNγ-secreting activated cytotoxic $CD8^+$ T cells of all splenocytes was determined by flow cytometry (Fig. 7A). The results showed that MSN-CD40/OVA/CpG nanoparticles induced intracellular secretion of IFNγ in splenocytes (Fig. 7B). The splenocytes were restimulated with $OVA_{257-264}$ peptide to acquire CTL effectors. The ELISA results revealed that MSN-CD40/OVA/CpG nanoparticles induced cytotoxic $CD8^+$ T cells to secrete IFNγ (Fig. 7C). Because the lymphatic system is the main site where the DCs interact with T cells, we excised the lymph nodes from immunized mice and tested the DC surface molecules. The results showed that MSN-CD40/OVA/CpG nanoparticles induced the DC maturation markers MHC-II, CD80, and CD86 compared with the indicated controls (Figs. 7D,E).

3.5 Antitumor efficacy in vivo

Activation of tumor-associated antigen-specific $CD8^+$ T cells is vital to elicit a robust anti-tumor immune response. Therefore, in this study, C57BL/6 mice were subcutaneously injected with B16-OVA cells and treated with MSN-CD40/OVA/CpG nanoparticles or appropriate controls containing the same doses of OVA and CpG, as described in the Methods and Fig. 8A. There were no differences in the body weights of mice in each group (Fig. 8C), indicating no obvious toxicity of the nanoparticles. Tumor growth was inhibited in mice immunized with MSN-CD40/OVA/CpG nanoparticles compared with that in mice immunized with MSN-IgG/OVA/CpG nanoparticles, MSN-OVA/CpG nanoparticles, free OVA/CpG, or saline (Figs. 8B,D). We also excised the tumor from each mouse and stained it with antibodies for $CD4^+$ and $CD8^+$ T cells for flow cytometry. The results showed that MSN-CD40/OVA/CpG nanoparticles increased

the frequency of $CD45^+CD3^+CD8^+$ and $CD45^+CD3^+CD4^+$ T infiltrating tumor cells (Figs. 9A,B). The spleen and lymph nodes were excised from tumor-bearing mice to detect intracellular IFNγ in splenocytes and lymphocytes (Figs. 9C,D). The MSN-CD40/OVA/CpG nanoparticles upregulated intracellular IFNγ production in splenocytes and lymphocytes to a greater extent than was observed in the other groups. Histopathological examination of the heart, liver, kidneys, and tumor (Fig. 10) revealed that the MSN-CD40/OVA/CpG nanoparticles were safe as a biomaterial.

4. Discussion

Prior clinical studies have evaluated vaccines in various conditions, including high expression of TCR and high affinity of T cells for phosphorylated MHCs expressed on tumor cells; high levels of granzymes and perforin;[3, 32] expression of cell surface molecules that promote T cell migration to the tumor site;[33] and high expression of costimulatory mediators or weakly expressed inhibitory molecules, such as cytotoxic T-lymphocyte-associated protein 4[34] and programmed cell death protein 1.[35] Activation of $CD8^+$ T cells is dependent on APCs for antigen presentation,[36, 37] whereas $CD4^+$ T cells produce cytokines that facilitate $CD8^+$ T cell proliferation and differentiation.[38]

DCs are involved in the capture, processing, and presentation of antigens to T cells, and hence play important roles in the effects of vaccines. Although peripheral tissue DCs can efficiently capture antigens,[39] they may induce immune tolerance during antigen presentation because of the lack of costimulatory mediators.[40, 41] Mature DCs can induce antigen-specific T cell differentiation to function as effector T cells. The maturation of DCs involves a variety of cellular changes, including decreased antigen uptake capacity; increased cell surface expression of MHC-II and costimulatory mediators; increased expression of chemokine receptors;[42] and cytokine secretion. Immune adjuvants can promote DC maturation. The effective anti-tumor responses elicited by DC vaccines depends the delivery of the tumor antigens to the DCs to induce tumor-specific CD8+ T cell responses. However, most vaccines are cleared from the body after subcutaneous injection. In this study, we designed and synthesized a DC-based nanovaccine, comprising CD40 mAb-modified MSNs, which was loaded with the model antigen OVA and the immuno-adjuvant CpG. MSN-CD40/OVA/CpG was designed to target and activate DC, inducing potent cytotoxic $CD8^+$ T cell responses. The MSN-CD40/OVA/CpG nanoparticles detected by FT-IR and TEM have a particle size of about 120 nm. The DLS results showed that the dispersibility of the prepared MSN-CD40/OVA/CpG nanoparticles was good (Fig. 1). Because CD40 is expressed on DC, B cells, and monocytes, the MSN-CD40/OVA-FITC/CpG nanoparticles could target different subpopulations of splenocytes. Our experiments revealed that the nanoparticles were specifically internalized by the DCs and B cells, but avoided non-specific phagocytosis by macrophages (Fig. 2). This specific targeting is a key advantage of the nanoparticles. B cells not only exert specific humoral immune functions by producing antibodies, but are also important APCs. The B cell-mediated immune responses, which depends on the antigen, can be divided into T cell-dependent antigen (TD-Ag) immune responses and T cell-independent antigen (TI-Ag) immune responses. It was previously reported that an antigen-loaded calcium phosphate (CaP) nanovaccine effectively activates B cells.[43] The CaP nanovaccine, which relies

on the function of the TLR ligand, can target B cells, promote their proliferation and differentiation, enhance and regulate the TI-Ag and TD-Ag responses, and enhance the humoral immune response.[44] However, because B cells display weaker phagocytic activity[45] and T cell activation,[46] than DC, B cells play a minor role in the effects of the nanovaccine.

To investigate the delivery of nanoparticles into DCs, OVA was labeled with fluorescent dye (FITC) and used to form the MSN-CD40/OVA-FITC/CpG complex. The MSN-CD40/OVA-FITC/CpG nanoparticles were co-incubated with BMDCs, allowing us to determine the mean FITC fluorescence in the cells. The mean fluorescence of cells incubated with MSN-CD40/OVA-FITC/CpG nanoparticles was significantly different from that in the control groups (Figs. 3A,B). To validate the endocytic mechanism of MSN-CD40/OVA-FITC/CpG nanoparticles by BMDCs, we exposed the cells with the caveolar endocytosis inhibitor genistein[47] and the clathrin-mediated endocytosis inhibitor chlorpromazine.[48] The results showed that chlorpromazine (10 μg/mL) effectively inhibited BMDC uptake of MSN-CD40/OVA-FITC/CpG nanoparticles. Although the effect of genistein (50 μg/mL) was not statistically significant, flow cytometry showed a decrease in the mean FITC fluorescence. Therefore, we concluded that BMDCs take up MSN-CD40/OVA-FITC/CpG nanoparticles through multiple pathways. TLR9 is localized in the endoplasmic reticulum rather than the cell surface.[49] Because the MSN-CD40/OVA/CpG nanoparticles enter DC via multiple pathways, they may also be useful to potentiate the activity of CpG oligodeoxynucleotides.[50-52]

The MSN-CD40/OVA/CpG nanoparticles greatly enhanced the maturation of BMDCs in vitro. Incubating BMDCs with MSN-CD40/OVA/CpG nanoparticles for 24 h resulted in marked upregulation of the cell surface molecules CD80 and CD86 compared with the control conditions. ELISA also revealed increased expression of TNFα, and the MTT assay showed that the nanoparticles had no toxic effects (Fig. 5F). We also evaluated antigen-specific $CD8^+$ T cells from OT-I mice and stained them with CFSE. Flow cytometry showed that the MSN-CD40/OVA/CpG nanoparticles induced $CD8^+$ T cell proliferation (Fig. 6A) and increased IFNγ secretion (Fig. 6B). These results indicate that the MSN-CD40/OVA/CpG nanoparticles promoted BMDC antigen cross-presentation, and induced antigen-specific $CD8^+$ T cell proliferation and activation.

When administered in vivo, the MSN-CD40/OVA/CpG nanoparticles induced significant DC maturation at the draining lymph node after three subcutaneous injections. The nanoparticles also induced the expression of the costimulatory markers CD80 and CD86, and of MHC-II (Figs. 7D,E). Furthermore, the nanoparticles stimulated the intracellular expression and secretion of IFNγ compared with the control conditions. Restimulation of splenocytes with $OVA_{257-264}$ also enhanced IFNγ secretion (Figs. 7B,C).

To investigate the antitumor effect of MSN-CD40/OVA/CpG nanoparticles, we established a B16-OVA-bearing mouse model (Fig. 8A). Three subcutaneous injections of the nanoparticles resulted in a decrease in tumor volume without a change in the body weight of the treated mice (Figs. 8B,C). Flow cytometry revealed upregulation of tumor-infiltrating $CD4^+$ T cells and $CD8^+$ T cells together with

increased intracellular IFNγ production (Figs. 9A,D). The systemic toxicity of anti-CD40 mAb can be reduced by using formulations that sequester the CD40 agonist in the tumor.[31, 53] To test this, we harvested the heart, liver, kidney, and tumor tissues from the treated mice and histopathologic staining with hematoxylin and eosin revealed no obvious inflammation or adverse pathology (Fig. 9E). These results suggested that MSN-CD40 is a safe, potential vaccine carrier.

5. Conclusion

In conclusion, we used anti-CD40 mAb to target DCs by covalently attaching the mAb to the surface of MSNs, which were then encapsulated with OVA and the TLR9 agonist CpG. The resulting MSN-CD40/OVA/CpG nanoparticles were efficiently taken up by DCs to induce their DC and antigen presentation, activating $CD8^+$ T cells in vitro and in vivo. We believe this represents a promising strategy to improve antigen cross-presentation, CTL immune activity, and antitumor immunotherapy.

Abbreviations

MSN, mesoporous silica nanoparticles

mAb, monoclonal antibody

OVA, ovalbumin

IFNγ, interferon γ

CTL, cytotoxic T lymphocytes

MHC, major histocompatibility complex

mDC, mature dendritic cells

iDC, immature dendritic cells

S.C., subcutaneous injection

Declarations

Ethics approval and consent to participate

The animal experiments conducted strictly in line with the Animal Study Guidelines of Zhengzhou University.

Consent for publication

All authors have agreed to the publication of the article.

Availability of data and material

All data and materials supporting the findings of this study are available from the corresponding author on reasonable request.

Competing interests

The authors have declared that no conflict of interest exists.

Funding

This work was financed by the National Natural Science Foundation of China (U1704174, U1604286 and 81601450) and development fund for outstanding young teachers of Zhengzhou University (1521311059).

Authors' contribution

Yajing Liu performed experiments, analyzed data and wrote the paper; Lintong Yao, Yun Zhang, Wenhui Shen, Chunxia Chen, and Hong fei Wang performed experiments and analyzed data; Yanfeng Gao and Yuanming Qi analyzed data; Zhenzhen Chen initiated the study, designed experiments and wrote the paper.

Acknowledgements

NA.

References

1. Rosenberg SA, Yang JC, Restifo NP. Cancer immunotherapy: moving beyond current vaccines. *Nat Med.* Sep 2004;10(9):909-915.
2. Mellman I, Coukos G, Dranoff G. Cancer immunotherapy comes of age. *Nature.* Dec 21 2011;480(7378):480-489.
3. Palucka K, Banchereau J. Dendritic-cell-based therapeutic cancer vaccines. *Immunity.* Jul 25 2013;39(1):38-48.
4. Tacken PJ, de Vries IJ, Torensma R, Figdor CG. Dendritic-cell immunotherapy: from ex vivo loading to in vivo targeting. *Nat Rev Immunol.* Oct 2007;7(10):790-802.
5. Zak DE, Aderem A. Systems integration of innate and adaptive immunity. *Vaccine.* Sep 29 2015;33(40):5241-5248.
6. Byrne KT, Vonderheide RH. CD40 therapy and surgery: a potential immunologic partnership. *J Immunother.* Sep 2013;36(7):359-361.
7. Beatty GL, Li Y, Long KB. Cancer immunotherapy: activating innate and adaptive immunity through CD40 agonists. *Expert Rev Anticancer Ther.* Feb 2017;17(2):175-186.

8. Schoenberger SP, Toes RE, van der Voort EI, Offringa R, Melief CJ. T-cell help for cytotoxic T lymphocytes is mediated by CD40-CD40L interactions. *Nature.* Jun 4 1998;393(6684):480-483.
9. Schuurhuis DH, Laban S, Toes RE, et al. Immature dendritic cells acquire CD8(+) cytotoxic T lymphocyte priming capacity upon activation by T helper cell-independent or -dependent stimuli. *J Exp Med.* Jul 3 2000;192(1):145-150.
10. Pasare C, Medzhitov R. Toll-like receptors: linking innate and adaptive immunity. *Adv Exp Med Biol.* 2005;560:11-18.
11. Min Y, Roche KC, Tian S, et al. Antigen-capturing nanoparticles improve the abscopal effect and cancer immunotherapy. *Nat Nanotechnol.* Sep 2017;12(9):877-882.
12. Zhang Z, Tongchusak S, Mizukami Y, et al. Induction of anti-tumor cytotoxic T cell responses through PLGA-nanoparticle mediated antigen delivery. *Biomaterials.* May 2011;32(14):3666-3678.
13. Zaric M, Lyubomska O, Touzelet O, et al. Skin dendritic cell targeting via microneedle arrays laden with antigen-encapsulated poly-D,L-lactide-co-glycolide nanoparticles induces efficient antitumor and antiviral immune responses. *ACS Nano.* Mar 26 2013;7(3):2042-2055.
14. Zhang P, Chiu YC, Tostanoski LH, Jewell CM. Polyelectrolyte Multilayers Assembled Entirely from Immune Signals on Gold Nanoparticle Templates Promote Antigen-Specific T Cell Response. *ACS Nano.* Jun 23 2015;9(6):6465-6477.
15. van Broekhoven CL, Parish CR, Demangel C, Britton WJ, Altin JG. Targeting dendritic cells with antigen-containing liposomes: a highly effective procedure for induction of antitumor immunity and for tumor immunotherapy. *Cancer Res.* Jun 15 2004;64(12):4357-4365.
16. Park J, Wrzesinski SH, Stern E, et al. Combination delivery of TGF-beta inhibitor and IL-2 by nanoscale liposomal polymeric gels enhances tumour immunotherapy. *Nat Mater.* Oct 2012;11(10):895-905.
17. Moon JJ, Suh H, Li AV, Ockenhouse CF, Yadava A, Irvine DJ. Enhancing humoral responses to a malaria antigen with nanoparticle vaccines that expand Tfh cells and promote germinal center induction. *Proc Natl Acad Sci U S A.* Jan 24 2012;109(4):1080-1085.
18. Gordon R. Individuation in the developmental process. *J Anal Psychol.* Jul 1986;31(3):223-230.
19. Li Y, Liu C. Nanomaterial-based bone regeneration. *Nanoscale.* Apr 13 2017;9(15):4862-4874.
20. Li J, Wang H, Yang B, et al. Control-release microcapsule of famotidine loaded biomimetic synthesized mesoporous silica nanoparticles: Controlled release effect and enhanced stomach adhesion in vitro. *Mater Sci Eng C Mater Biol Appl.* Jan 1 2016;58:273-277.
21. Shao Y, Sun ZY, Wang Y, Zhang BD, Liu D, Li YM. Designable Immune Therapeutical Vaccine System Based on DNA Supramolecular Hydrogels. *ACS Appl Mater Interfaces.* Mar 21 2018;10(11):9310-9314.
22. Kuai R, Ochyl LJ, Bahjat KS, Schwendeman A, Moon JJ. Designer vaccine nanodiscs for personalized cancer immunotherapy. *Nat Mater.* Apr 2017;16(4):489-496.

23. Phuengkham H, Song C, Um SH, Lim YT. Implantable Synthetic Immune Niche for Spatiotemporal Modulation of Tumor-Derived Immunosuppression and Systemic Antitumor Immunity: Postoperative Immunotherapy. *Adv Mater.* May 2018;30(18):e1706719.
24. Xiang J, Xu L, Gong H, et al. Antigen-Loaded Upconversion Nanoparticles for Dendritic Cell Stimulation, Tracking, and Vaccination in Dendritic Cell-Based Immunotherapy. *ACS Nano.* Jun 23 2015;9(6):6401-6411.
25. Hu JJ, Xiao D, Zhang XZ. Advances in Peptide Functionalization on Mesoporous Silica Nanoparticles for Controlled Drug Release. *Small.* Jul 2016;12(25):3344-3359.
26. Cohn L, Chatterjee B, Esselborn F, et al. Antigen delivery to early endosomes eliminates the superiority of human blood BDCA3+ dendritic cells at cross presentation. *J Exp Med.* May 6 2013;210(5):1049-1063.
27. Schjetne KW, Fredriksen AB, Bogen B. Delivery of antigen to CD40 induces protective immune responses against tumors. *J Immunol.* Apr 1 2007;178(7):4169-4176.
28. van Mierlo GJ, den Boer AT, Medema JP, et al. CD40 stimulation leads to effective therapy of CD40(-) tumors through induction of strong systemic cytotoxic T lymphocyte immunity. *Proc Natl Acad Sci U S A.* Apr 16 2002;99(8):5561-5566.
29. Tutt AL, O'Brien L, Hussain A, Crowther GR, French RR, Glennie MJ. T cell immunity to lymphoma following treatment with anti-CD40 monoclonal antibody. *J Immunol.* Mar 15 2002;168(6):2720-2728.
30. Retraction. Pharmacogenomic strategies provide a rational approach to the treatment of cisplatin-resistant patients with advanced cancer. J Clin Oncol 25:4350-7, 2007. *J Clin Oncol.* Dec 10 2010;28(35):5229.
31. Fransen MF, Sluijter M, Morreau H, Arens R, Melief CJ. Local activation of CD8 T cells and systemic tumor eradication without toxicity via slow release and local delivery of agonistic CD40 antibody. *Clin Cancer Res.* Apr 15 2011;17(8):2270-2280.
32. Appay V, Douek DC, Price DA. CD8+ T cell efficacy in vaccination and disease. *Nat Med.* Jun 2008;14(6):623-628.
33. Mullins IM, Slingluff CL, Lee JK, et al. CXC chemokine receptor 3 expression by activated CD8+ T cells is associated with survival in melanoma patients with stage III disease. *Cancer Res.* Nov 1 2004;64(21):7697-7701.
34. Peggs KS, Quezada SA, Chambers CA, Korman AJ, Allison JP. Blockade of CTLA-4 on both effector and regulatory T cell compartments contributes to the antitumor activity of anti-CTLA-4 antibodies. *J Exp Med.* Aug 3 2009;206(8):1717-1725.
35. Freeman GJ, Wherry EJ, Ahmed R, Sharpe AH. Reinvigorating exhausted HIV-specific T cells via PD-1-PD-1 ligand blockade. *J Exp Med.* Oct 2 2006;203(10):2223-2227.
36. Joffre OP, Segura E, Savina A, Amigorena S. Cross-presentation by dendritic cells. *Nat Rev Immunol.* Jul 13 2012;12(8):557-569.

37. Lizee G, Overwijk WW, Radvanyi L, Gao J, Sharma P, Hwu P. Harnessing the power of the immune system to target cancer. *Annu Rev Med.* 2013;64:71-90.
38. Spolski R, Leonard WJ. Interleukin-21: basic biology and implications for cancer and autoimmunity. *Annu Rev Immunol.* 2008;26:57-79.
39. Mellman I, Steinman RM. Dendritic cells: specialized and regulated antigen processing machines. *Cell.* Aug 10 2001;106(3):255-258.
40. Takenaka MC, Quintana FJ. Tolerogenic dendritic cells. *Semin Immunopathol.* Feb 2017;39(2):113-120.
41. Tarbell KV, Petit L, Zuo X, et al. Dendritic cell-expanded, islet-specific CD4+ CD25+ CD62L+ regulatory T cells restore normoglycemia in diabetic NOD mice. *J Exp Med.* Jan 22 2007;204(1):191-201.
42. Steinman RM, Banchereau J. Taking dendritic cells into medicine. *Nature.* Sep 27 2007;449(7161):419-426.
43. Temchura VV, Kozlova D, Sokolova V, Uberla K, Epple M. Targeting and activation of antigen-specific B-cells by calcium phosphate nanoparticles loaded with protein antigen. *Biomaterials.* Jul 2014;35(23):6098-6105.
44. Zilker C, Kozlova D, Sokolova V, et al. Nanoparticle-based B-cell targeting vaccines: Tailoring of humoral immune responses by functionalization with different TLR-ligands. *Nanomedicine.* Jan 2017;13(1):173-182.
45. Rabinovitch M. Professional and non-professional phagocytes: an introduction. *Trends Cell Biol.* Mar 1995;5(3):85-87.
46. Lim TS, Goh JK, Mortellaro A, Lim CT, Hammerling GJ, Ricciardi-Castagnoli P. CD80 and CD86 differentially regulate mechanical interactions of T-cells with antigen-presenting dendritic cells and B-cells. *PLoS One.* 2012;7(9):e45185.
47. Aoki T, Nomura R, Fujimoto T. Tyrosine phosphorylation of caveolin-1 in the endothelium. *Exp Cell Res.* Dec 15 1999;253(2):629-636.
48. Wang LH, Rothberg KG, Anderson RG. Mis-assembly of clathrin lattices on endosomes reveals a regulatory switch for coated pit formation. *J Cell Biol.* Dec 1993;123(5):1107-1117.
49. Blasius AL, Beutler B. Intracellular toll-like receptors. *Immunity.* Mar 26 2010;32(3):305-315.
50. Tao Y, Zhang Y, Ju E, Ren H, Ren J. Gold nanocluster-based vaccines for dual-delivery of antigens and immunostimulatory oligonucleotides. *Nanoscale.* Aug 7 2015;7(29):12419-12426.
51. de Titta A, Ballester M, Julier Z, et al. Nanoparticle conjugation of CpG enhances adjuvancy for cellular immunity and memory recall at low dose. *Proc Natl Acad Sci U S A.* Dec 3 2013;110(49):19902-19907.
52. Bourquin C, Anz D, Zwiorek K, et al. Targeting CpG oligonucleotides to the lymph node by nanoparticles elicits efficient antitumoral immunity. *J Immunol.* Sep 1 2008;181(5):2990-2998.
53. Kwong B, Liu H, Irvine DJ. Induction of potent anti-tumor responses while eliminating systemic side effects via liposome-anchored combinatorial immunotherapy. *Biomaterials.* Aug 2011;32(22):5134-

5147.

Figures

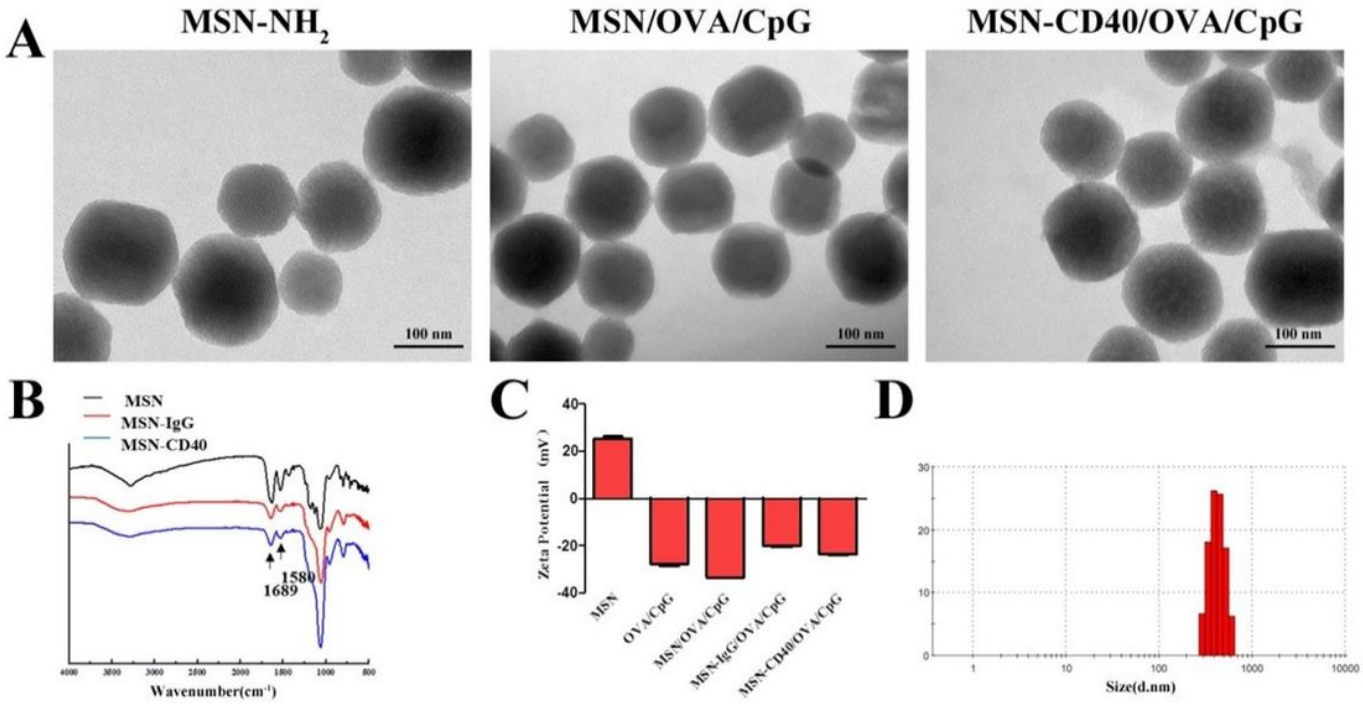

Figure 1

Characterization of the nanoparticles. TEM images of MSN-NH2, MSN/OVA/CpG, and MSN-CD40/OVA/CpG. Scale bar = 100 nm. (B) FT-IR spectra of MSN, IgG mAb-conjugated MSN (MSN-IgG), and CD40 mAb-conjugated MSNs (MSN-CD40). (C) Zeta potentials. (D) DLS of MSN-CD40/OVA/CpG.

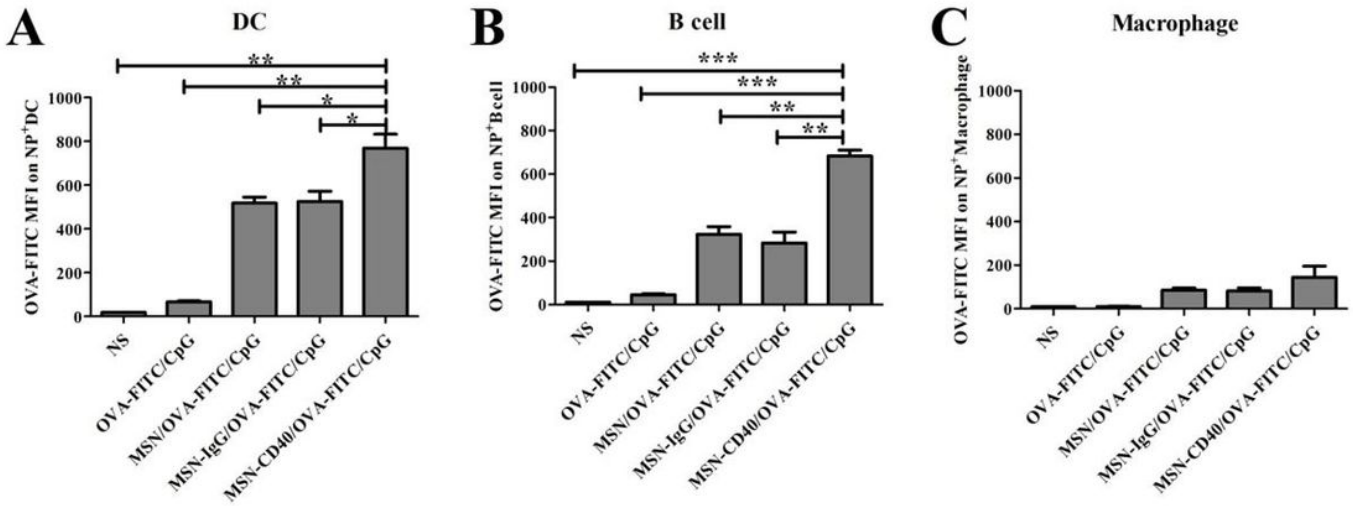

Figure 2

Capacity of MSN-CD40/OVA/CpG internalization by subsets of splenocytes from C57BL/6 mice. Splenocytes were incubated with OVA-FITC at a final concentration of 12.5 μg/mL in MSN-CD40/OVA/CpG or non-targeted nanoparticles for 4 h at 37 °C. The cells were stained with the indicated antibodies and analyzed by flow cytometry. The mean fluorescence values are shown for (A) CD45+CD11c+ DCs, (B) CD45+B220+CD19b+ B cells, and (C) CD45+F4/80+CD11b macrophages. The results are presented as the mean ± SD (n = 2). *P < 0.05, **P < 0.01, and ***P < 0.001.

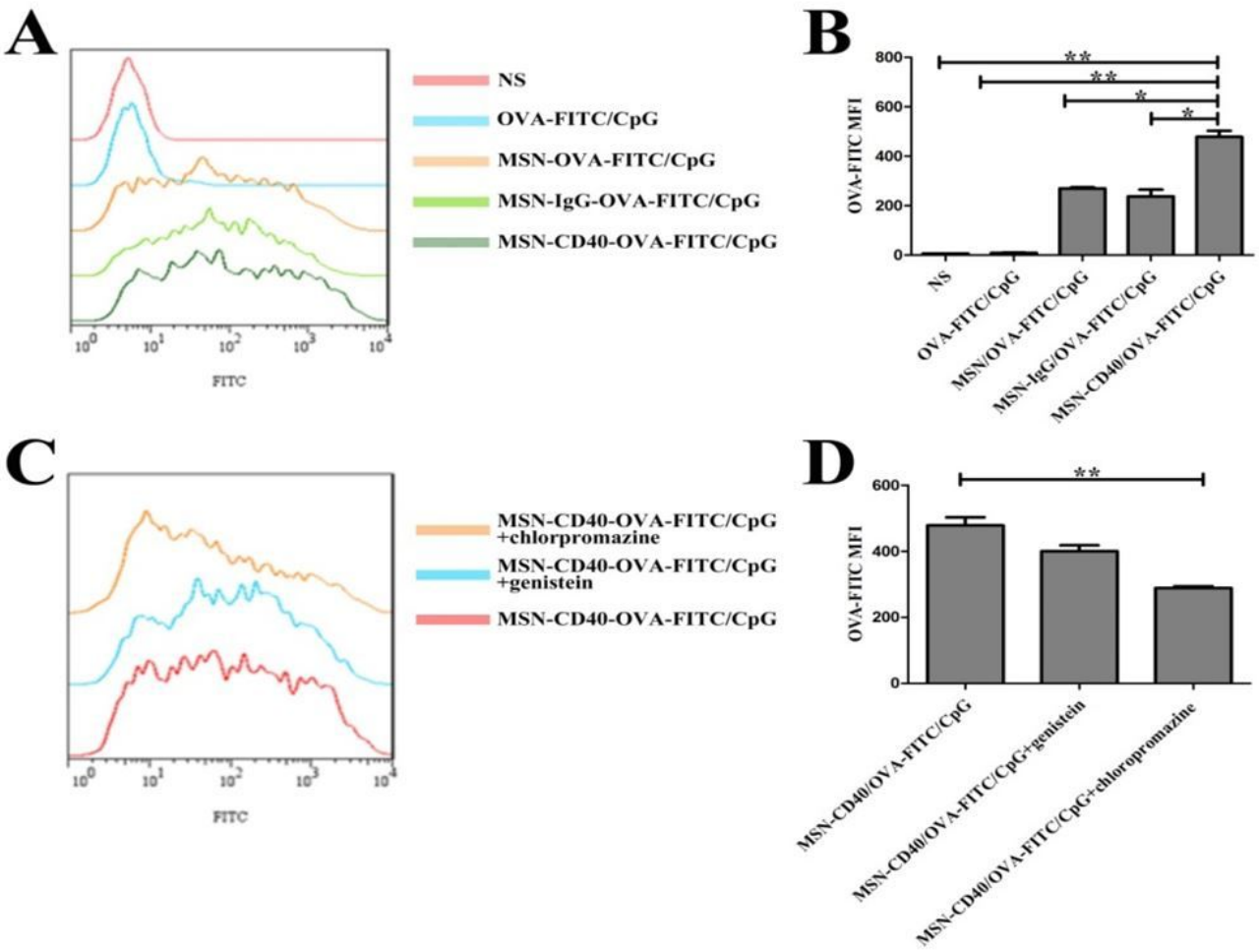

Figure 3

MSN-CD40/OVA/CpG nanoparticles enhance OVA-FITC uptake by BMDCs through multiple receptors. (A,C) BMDCs were incubated with OVA-FITC at a final concentration of 12.5 μg/mL in MSN-CD40/OVA/CpG or non-targeted nanoparticles for 4 h at 37 °C. (B,D) Inhibitory effects of genistein (50 μg/mL) or chlorpromazine (10 μg/mL) on OVA-FITC uptake via MSN-CD40/OVA/CpG. The cells were analyzed by flow cytometry. The relative number of particles internalized by BMDCs was determined by FITC fluorescence intensity. Results are presented as means ± SD (n = 2). *P < 0.05, **P < 0.01, and ***P < 0.001.

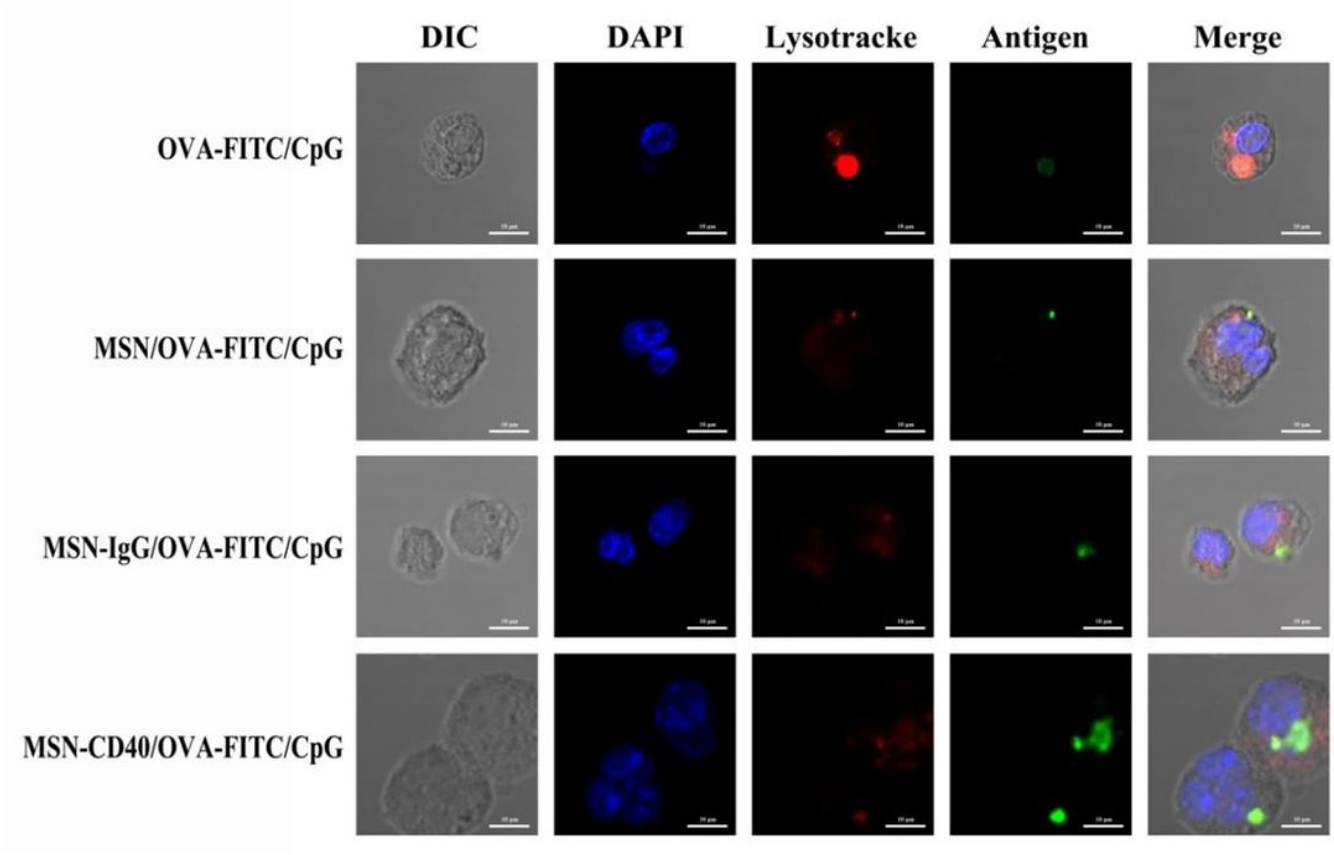

Figure 4

Confocal microscopic images of free OVA-FITC and BMDCs incubated with the nanoparticles. BMDCs were incubated with OVA-FITC at a final concentration of 12.5 μg/mL (green) in MSN-CD40/OVA/CpG nanoparticles or non-targeted nanoparticles for 4 h at 37 °C. The cells were then stained with Hoechst (blue) and Lysotracker (red). Scale bar = 7.5 μm.

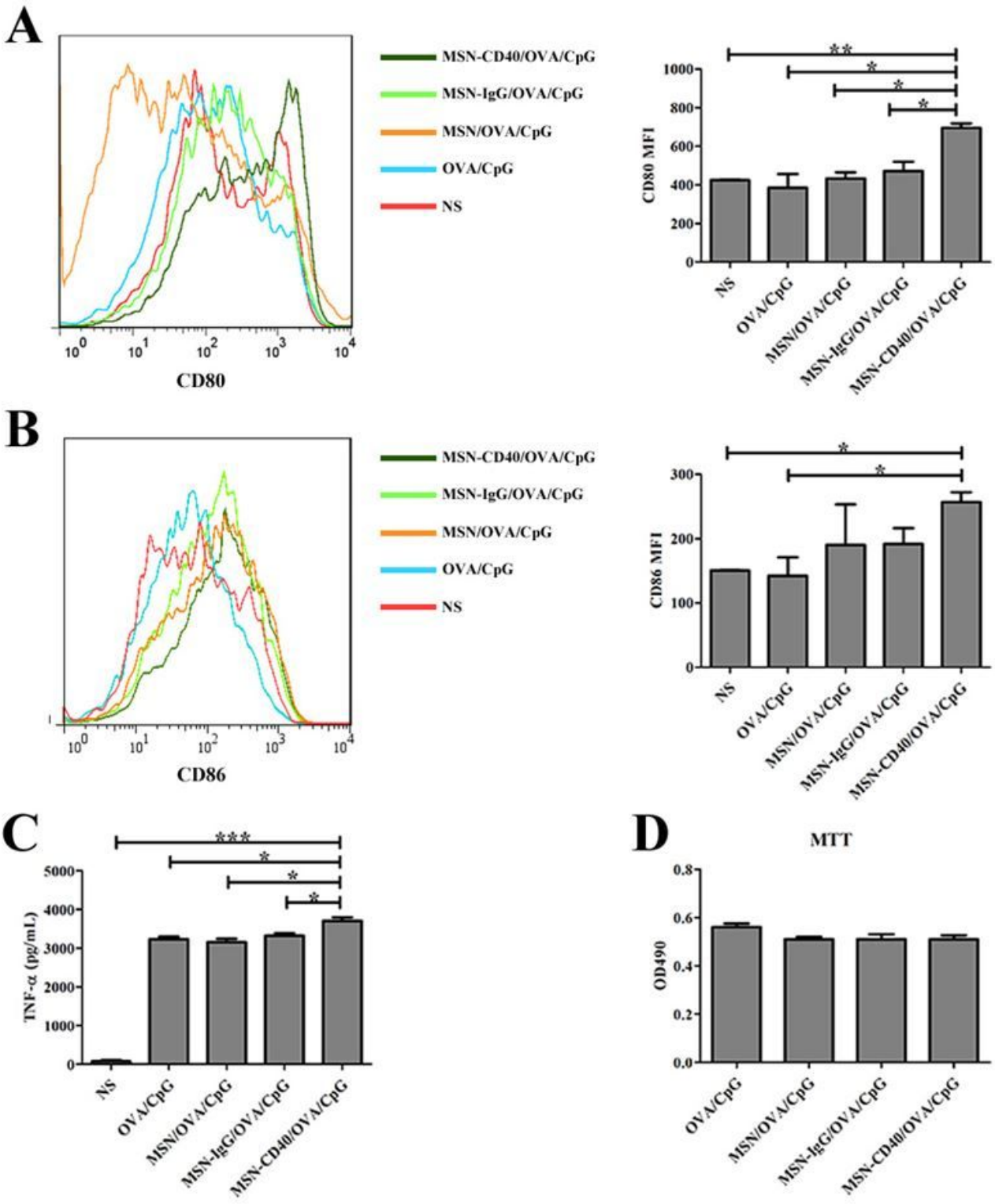

Figure 5

Characterization of BMDC maturation in vitro. BMDCs were incubated with OVA at a concentration of 12.5 μg/mL OVA and CpG at a concentration of 7.5 μg/mL in MSN-CD40/OVA/CpG nanoparticles or non-targeted nanoparticles for 24 h at 37 °C. BMDC expression of CD80 (A) and CD86 (B) was detected by flow cytometry. (C) IFNγ levels in the culture supernatant were measured by an ELISA. (D) MTT assay.

Cell activity was not affected by the nanoparticles. The results are presented as means ± SD (n = 2). *P < 0.05, **P < 0.01, and ***P < 0.001.

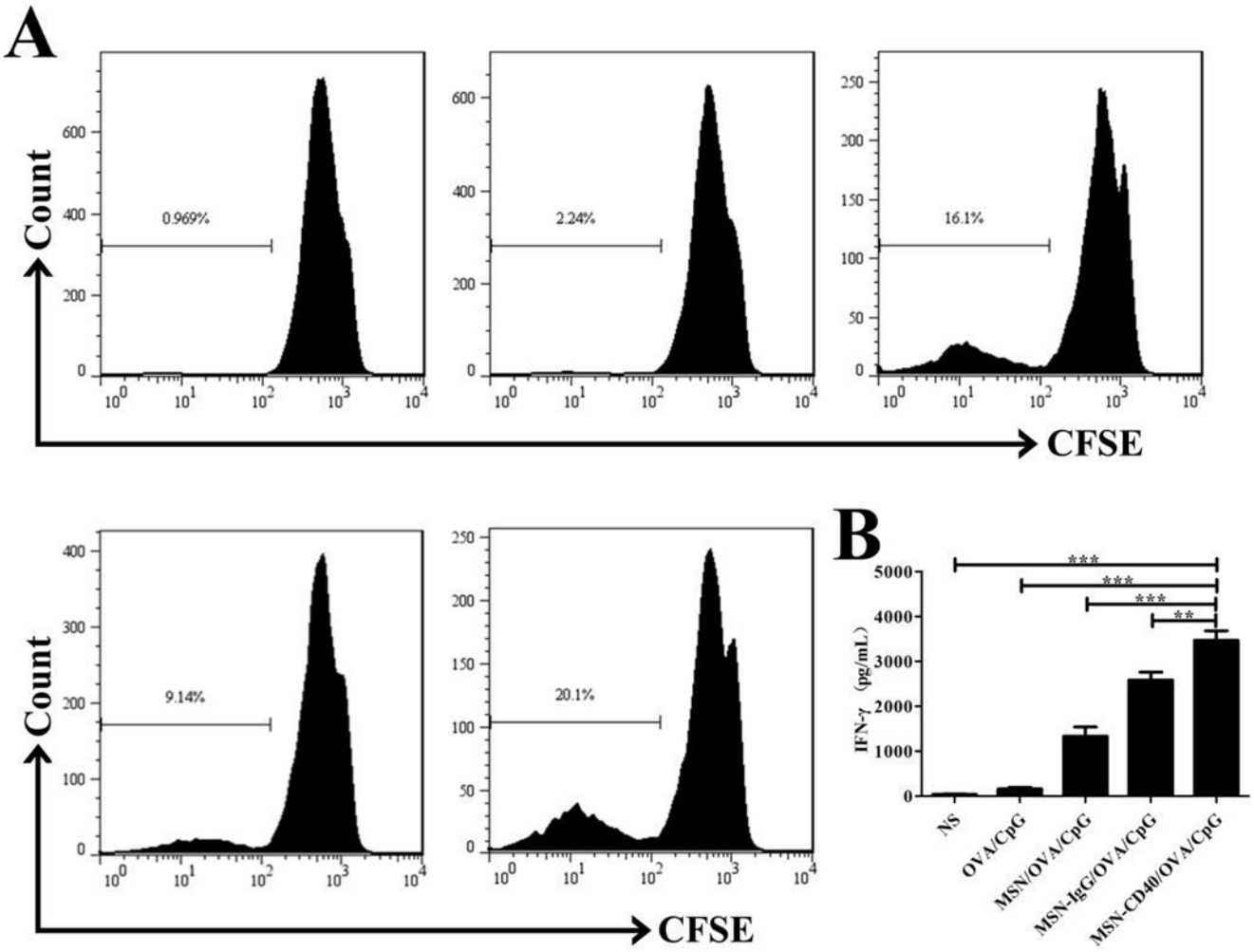

Figure 6

Effects of MSN-CD40/OVA/CpG nanoparticles on antigen cross-presentation by BMDCs in vitro. BMDCs were incubated with OVA at a concentration of 12.5 μg/mL and CpG at a concentration of 7.5 μg/mL in MSN-CD40/OVA/CpG nanoparticles or non-targeted nanoparticles. (A) CD8+ T cell proliferation. (B) IFNγ levels were measured by ELISA. The results are presented as means ± SD. *P < 0.05, **P < 0.01, and ***P < 0.001.

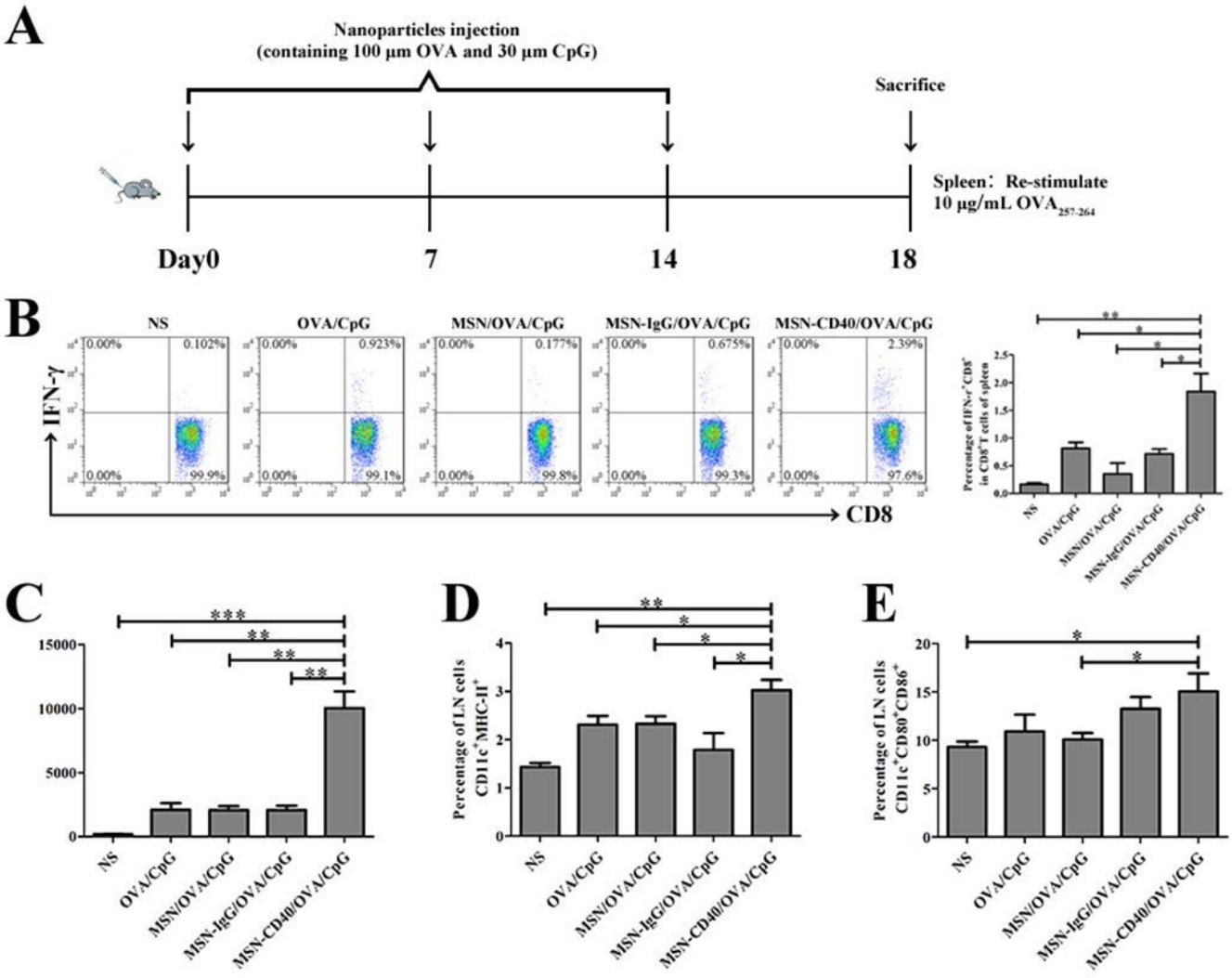

Figure 7

Effects of MSN-CD40/OVA/CpG nanoparticles on OVA257–264-specific CD8+ T cells in C57BL/6 mice. (A) Schematic of the mouse immunization as described in the Methods section with 100 μg of OVA and 30 μg of CpG into the tail base three times at 1 week intervals. The mice were sacrificed 5 days after the last immunization. The splenocytes were restimulated with OVA257–264 peptide for 6 h or 5 days at 37 °C in vitro. (B) Proportion of IFNγ-secreting cytotoxic CD8+ T cells of all splenocytes analyzed by flow cytometry. (C) IFNγ production measured by ELISA. (D,E) Analysis of DC maturation markers MHC-II (D) and CD80 and CD86 (E) in the lymphocytes after immunization with MSN-CD40/OVA/CpG or the indicated controls. The results are presented as means ± SD (n = 5). *P < 0.05, **P < 0.01, and ***P < 0.001.

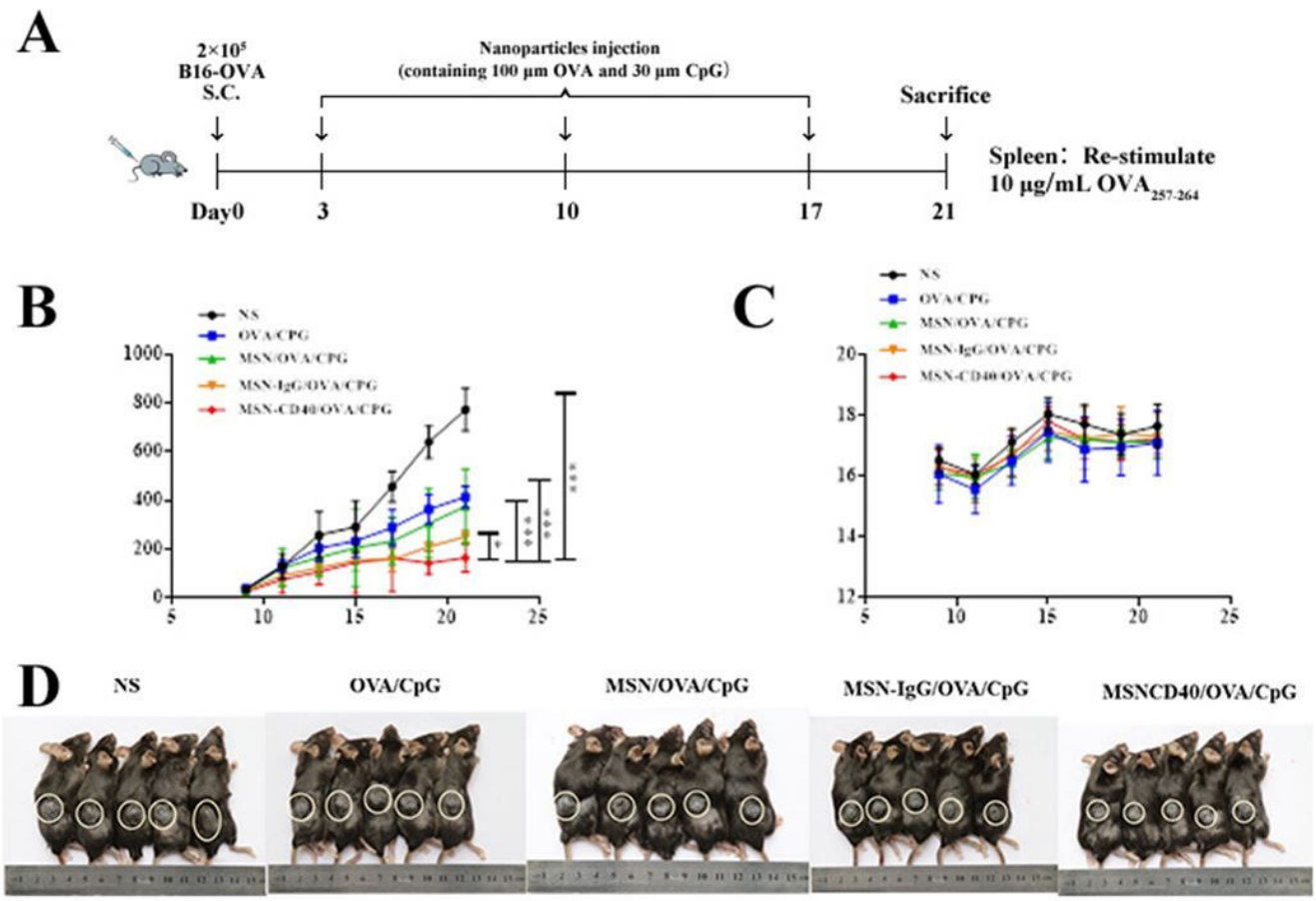

Figure 8

MSN-CD40/OVA/CpG nanoparticles display antitumor vaccine potency. (A) Schematic of the experiment. B16-OVA melanoma cells were injected into the left flank of C57BL/6 mice. On day 3, the mice were immunized with 100 μg OVA and 30 μg CpG in the tail base three times at 1-week intervals, and sacrificed 5 days after the last immunization. (B) Tumor volume and (C) body weight of each groups. (D) Photographs of the tumor-bearing mice. The results are presented as means ± SD (n = 5). *P < 0.05, **P < 0.01, and ***P < 0.001.

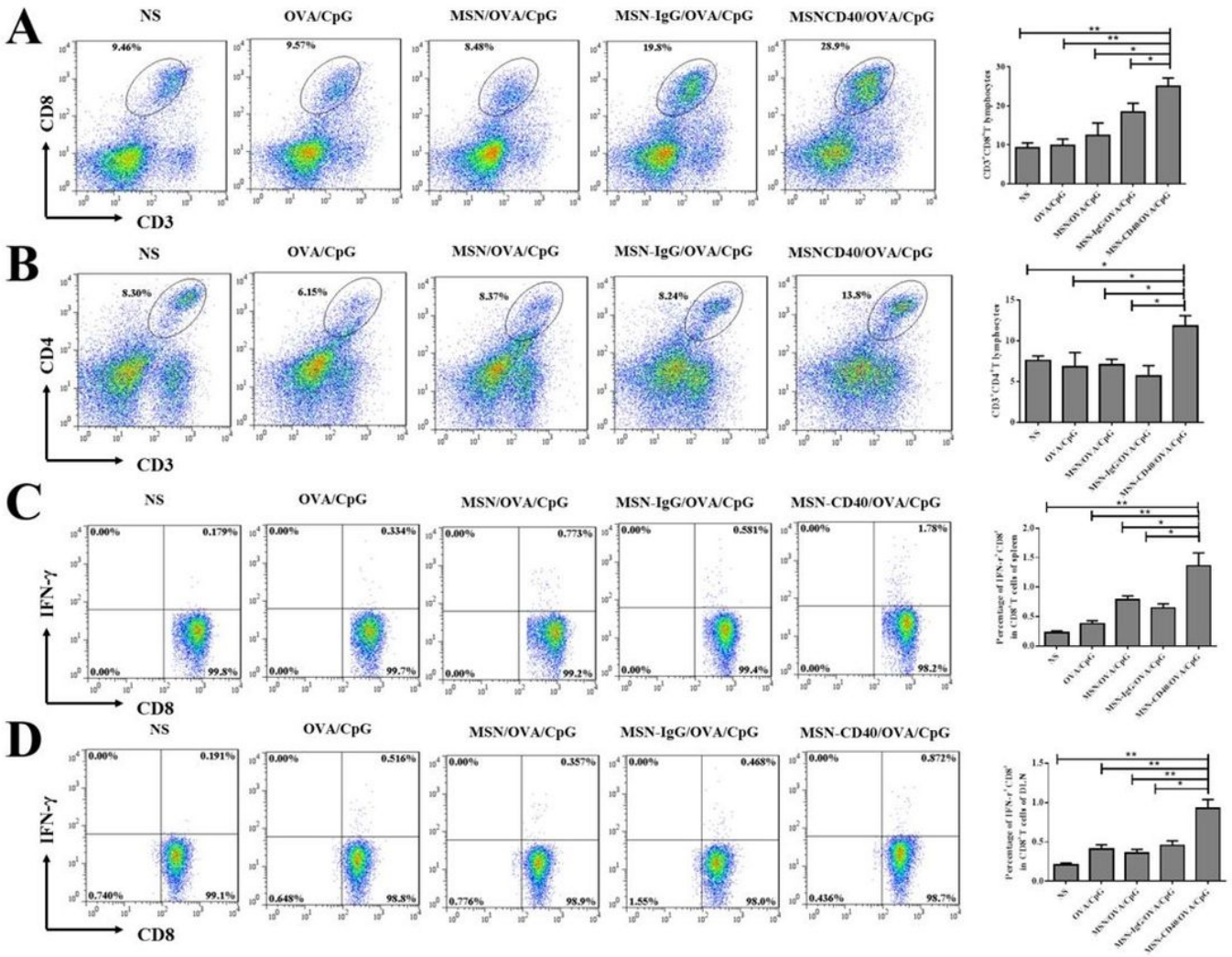

Figure 9

Anti-tumor vaccine potency of MSN-CD40/OVA/CpG nanoparticles. (A,B) Frequency of CD45+CD3+CD8+ (A) and CD45+CD3+CD4+ (B) T infiltrating tumor cells detected by flow cytometry. (C,D) Frequencies of IFNγ-secreting activated cytotoxic CD8+ T cells of splenocytes (C) and lymphocytes (D) analyzed by flow cytometry.

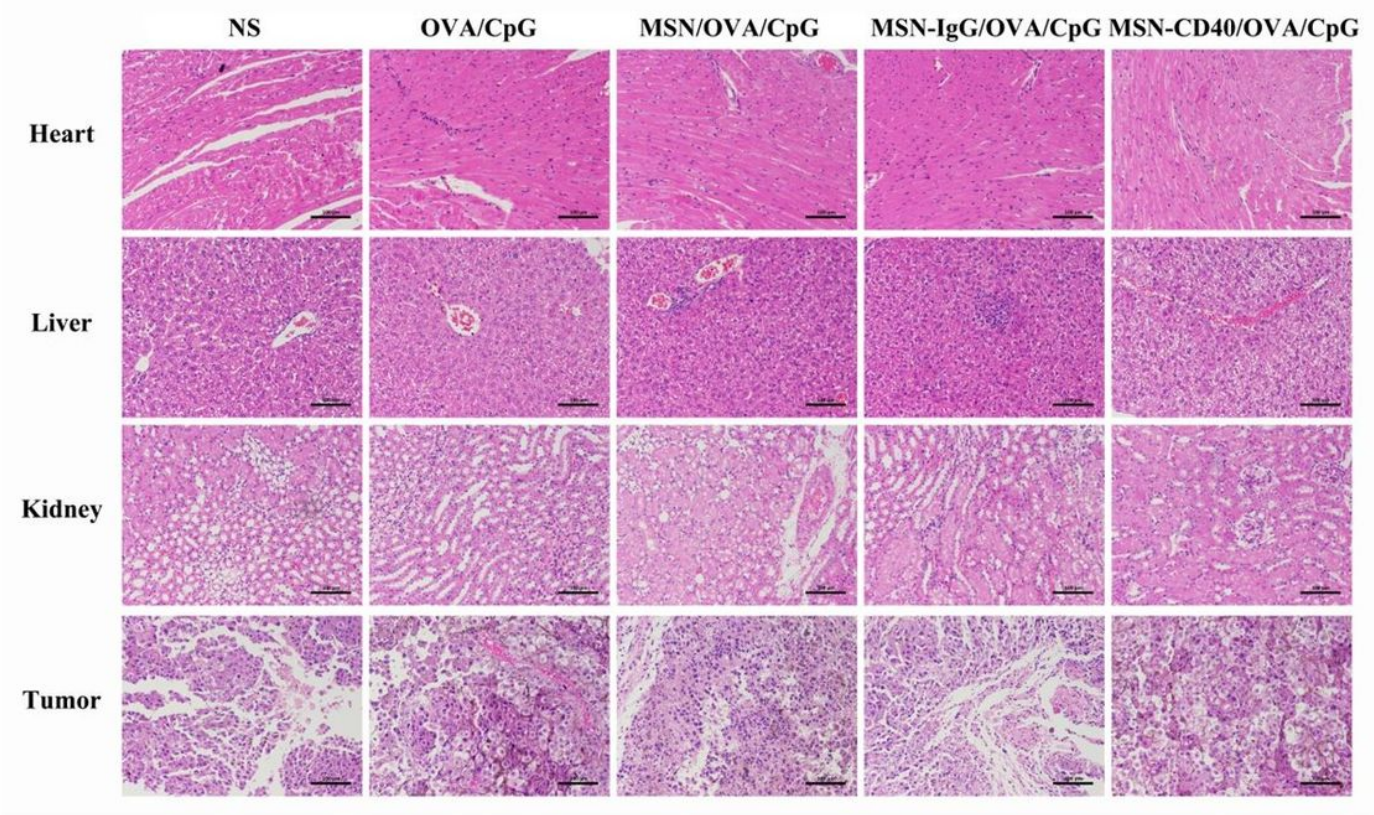

Figure 10

Hematoxylin and eosin staining of the heart, liver, kidney, and tumor tissues from tumor-bearing mice. Magnification, ×200. The results are presented as means ± SD (n = 5). *P < 0.05, **P < 0.01, and ***P < 0.001.

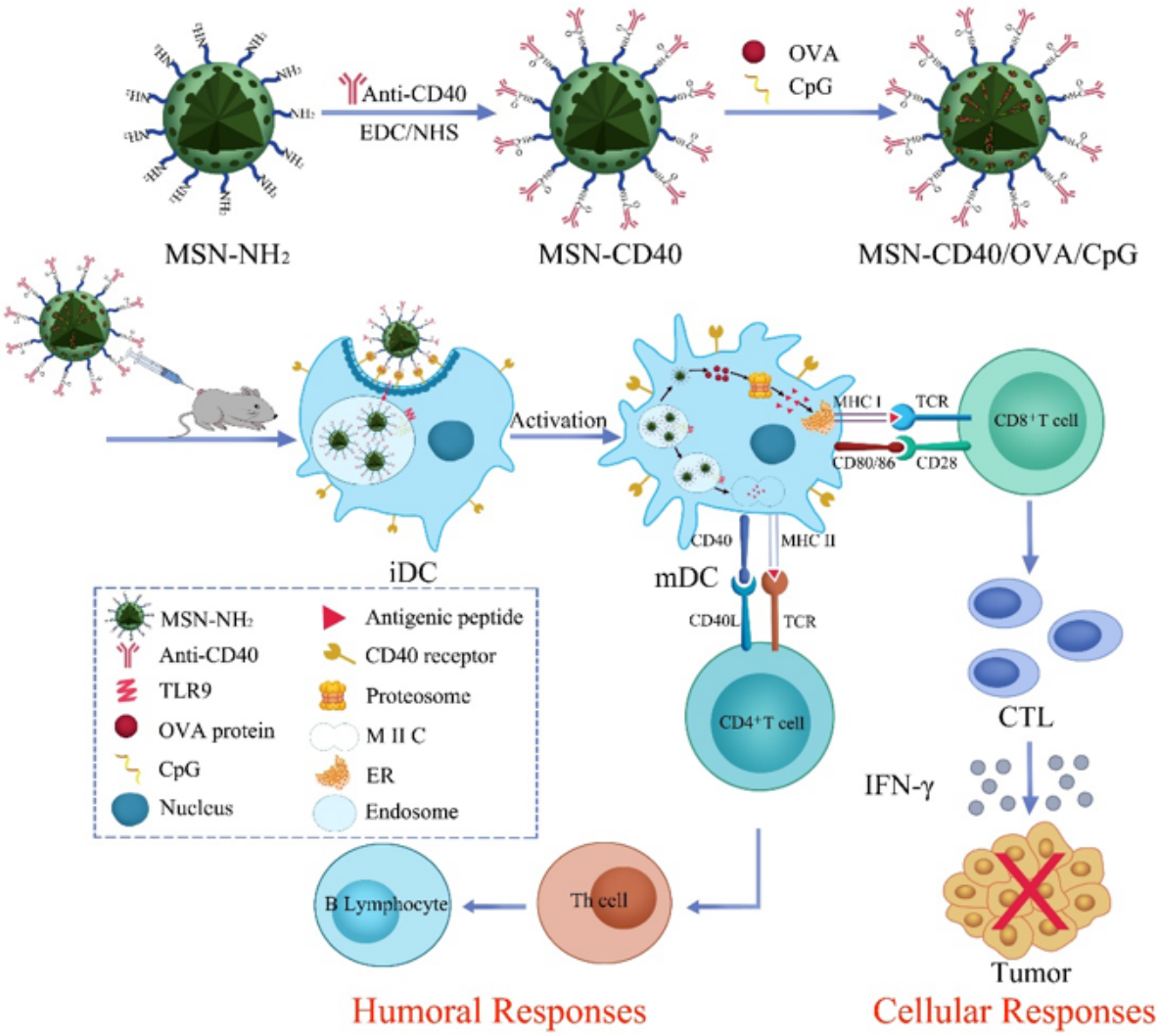

Figure 11

Scheme 1. Synthesis of MSN-CD40/OVA/CpG nanoparticles and immunotherapeutic potential.